Validation of Collisional Radiative Model of High-Z Multiple Charged Ions at NLTE Code Comparison Workshops*)

Akira SASAKI and Izumi MURAKAMI[1)]

Japan Atomic Energy Agency, Kyoto 619-0215, Japan
[1)]*National Institute for Fusion Science, Toki 509-5292, Japan*

(Received 14 December 2012 / Accepted 5 February 2013)

We develop a collisional radiative (CR) model of high-Z multiple charge ions based on computational atomic data. We use an algorithm to determine a set of atomic energy levels in the model with significant population in the plasmas and contribute to the dielectronic recombination (DR) processes. The model is validated through participation to the non-LTE kinetics workshops. At the nLTE workshop, an alternative method for the analysis of the spectrum from plasmas based on genetic algorithm (GA) is also discussed. An application of the present model to calculate the ion abundance and radiative power loss of Gd and Nd plasmas is also shown.

Keywords: atomic processes, collisional radiative model, tungsten, simulation

DOI: 10.1585/pfr.8.2401021

1. Introduction

Atomic processes in high-Z plasmas have attracted great interest in plasma science. Because tungsten (W) has potential as a plasma-facing material of divertor plates for ITER and future fusion reactors [1], collisional radiative (CR) models of tungsten are investigated. Similarly, atomic processes in Xe and Sn plasmas are investigated, which have potential as an EUV source for microlithography [2].

Because the multiple-charge ions of high-Z atom have a very complex structure, the development of the CR model has been a difficult subject. The model should include a large number of atomic states as well as a wide variety of collisional and radiative ionization and excitation processes. Recent development of atomic codes such as HULLAC [3] and FAC [4] has enabled one to develop such a CR model.

However, the CR model should be validated before its application to plasma spectroscopy. However, the emission spectrum from plasmas is complex and measurements are subject to spatial-temporal evolution of the plasmas, making validation through comparison between calculation and experiment difficult. Therefore, NLTE workshops are held since 1996. The activity of the workshops are extensively reported by Rubiano et. al [5] and Ralchenko et. al [6]. In these workshops participants share the results of their atomic kinetics codes for predetermined test problems, and codes are improved by comparing the calculated quantities such as mean charge, radiative power loss, ion abundance, and rates of ionization and recombination.

In this paper, we report the development of JATOM CR code and its validation via a calculation for W plasmas at recent NLTE7 workshop [7]. Additionally, we model the Kr spectrum based on the genetic algorithm (GA) as an alternative method to analyze atomic kinetics. Finally, we demonstrate a few applications of JATOM code.

2. Modeling Method

In the JATOM CR code, we employ the configuration average (CA) model, taking sufficiently large number of atomic states into account, including those with low excitation energy and have large population as well as those contribute to dielectronic recombination and affect the determination of ionization balance.

Figure 1 shows the atomic structure of the Ne- and Cl-like W ions used in the model. The set of energy levels is determined recursively descending ion charge, from the highest charged ion. For example, to produce the set of energy levels of Na-like ion, firstly, typically 30 lowest excited states of Ne-like ion, $2s^2 2p^5 nl$ and $2s2p^6 nl$ are selected. Secondly, the groups of excited states of Na-like ion, which terminate to the selected Ne-like states, $2s^2 2p^5 nln'l'$ and $2s2p^6 nln'l'$, and contribute to the dielectroic recombination are generated. Using the present algorithm, in the case of ions around W^{57+}, multiple M-shell excited states are rather preferred than those contribute more to the dielectronic recombination with n = 3-4 excitation of an electron. Regardless, the number of excited states of the source ion controls the size of the present model, which is decided after a convergence analysis of the mean charge and radiative power loss as described in the next section.

We use HULLAC code to calculate the energy levels, rates of radiative decay and autoionization in the CA mode

author's e-mail: akira.sasaki@jaea.go.jp
*) This article is based on the presentation at the 22nd International Toki Conference (ITC22).

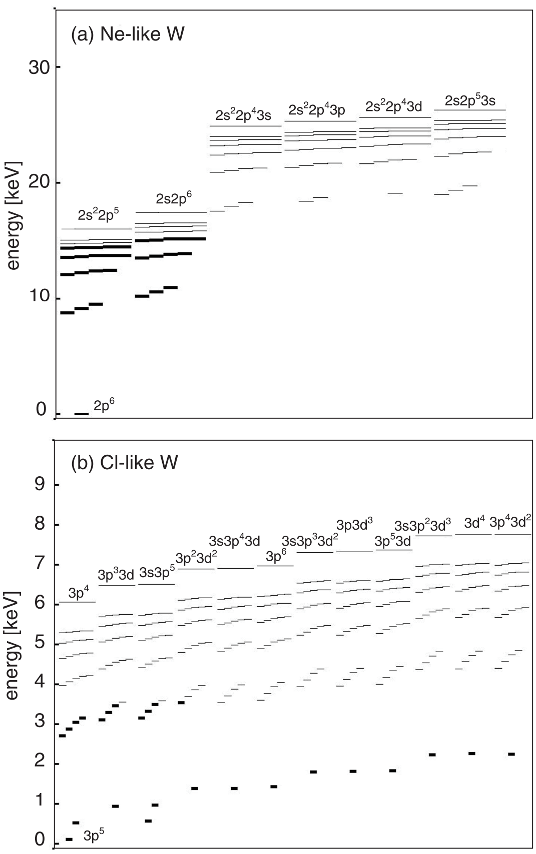

Fig. 1 Energy level diagram of (a) Ne- and (b) Cl-like W, Thick lines indicate excited states from which Na- or Ar-like ions are produced in the typical model which includes 30 groups of excited states for each ion.

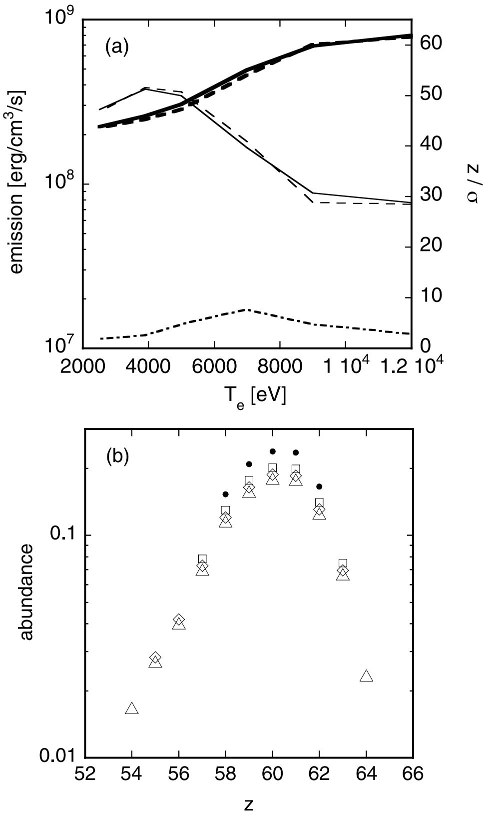

Fig. 2 (a) Mean charge [$\Delta = 2$ (thick dotted line), and 5 (thick solid line)], and radiative power loss [$\Delta = 2$ (thin dotted line), and 5 (thin solid line)] calculated with different window width. Second moment of mean charge is also shown (dash dotted line). (b) Abundance of each ion calculated with $\Delta = 2$ (closed circle), 3 (square), 4 (diamond) and 5 (triangle) .

without configuration interaction. The rates of other processes are calculated using empirical formulas as a function of the energy difference of initial and final state and the oscillator strength. Details of the model is described in elsewhere [8].

To calculate the level population of W ions over wide range of temperatures, we construct an atomic model from Gd- to H-like ions. However, at a specific temperature, only a relatively small number of charge states are populated. Therefore, the calculation uses a "sliding window" approach, in which only $(2\Delta + 1)$ ions around the most abundant one are considered at each temperature.

3. Results of Calculation Using JATOM

We carried out calculation of W plasmas with an electron density and temperature of $n_e = 10^{14}/\text{cm}^3$ and $T_e = 100 - 12000$ eV. The results depend on the number of groups of excited states, maximum principal quantum and angular moment quantum number of excited electron, and the number of ions considered in the calculation for each temperature, or the width of the sliding window. Therefore, we carried out convergence analyses.

Figure 2 shows dependence of the result with respect to the width of the sliding window. The abundance of each ion changes significantly depends on the window width, although the mean charge and radiative loss are less sensitive. We performed following calculations with $\Delta = 4$. The result suggests more ions should be included in such conditions where the open shell ions dominates. Furthermore, the mean charge and radiative power loss converge when excited states with the principal and angular momentum quantum number of the excited electron up to $n = 8$ and $l = 4$ are included.

Figure 3 compares the results of JATOM code with those presented at NLTE7 workshop. The calculated mean charge and radiative power loss are nearly at the center of the distribution, except for the radiative power loss at $T_e = 9000$ eV. Figure 3 also shows the results with fewer number of levels. As the size of the model increases, the mean charge decreases as the rates of dielectronic recombination increases, whereas the radiative power loss increases as the satellite line emission increases. These results indicate that including 30 groups of excited states for the calculation of mean charge are sufficient to calculate

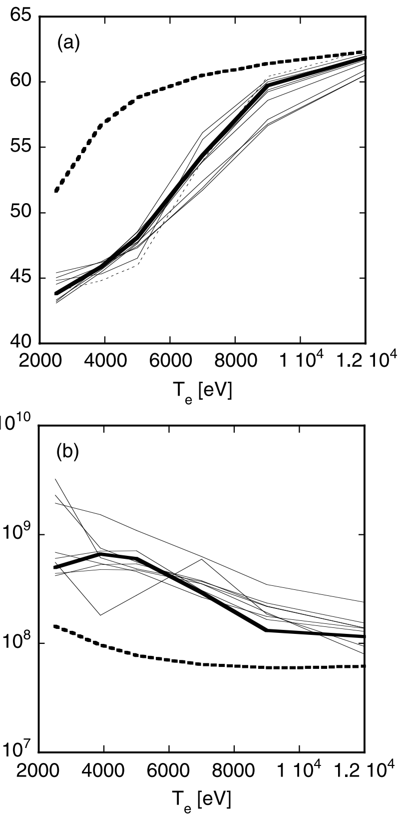

Fig. 3 (a) Mean charge and (b) radiative power loss of W plasmas at a density of $n_e = 10^{14}/\mathrm{cm}^3$. Thin lines correspond to the result presented at the NLTE7 workshop. Solid and dotted lines show the results of JATOM code with standard model with 30 groups and smaller model with 10 groups of excited states for each ion, respectively.

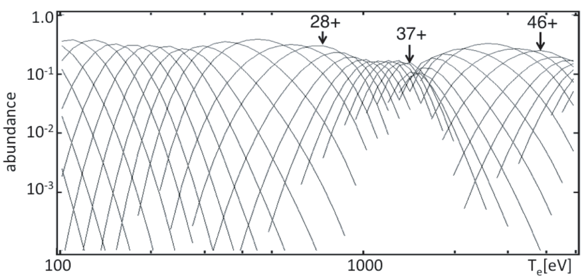

Fig. 4 Abundance of each ion of W, indicating abundance of Ni- (W^{46+}), Rb- (W^{37+}), and Pd- (W^{28+}) like ions.

the mean charge, However under such conditions when open M-shell ions are dominant, more $\Delta n \neq 0$ dielectronic recombination channels should be included otherwise the calculation may underestimate the emission.

Figure 4 shows the temperature dependent ion abundance of W. The calculated mean charge at $T_e = 3900\,\mathrm{eV}$ is $Z = 45$, which is similar to that reported by Pütterich [9], however, is higher at other temperatures, suggesting that further investigation may be required.

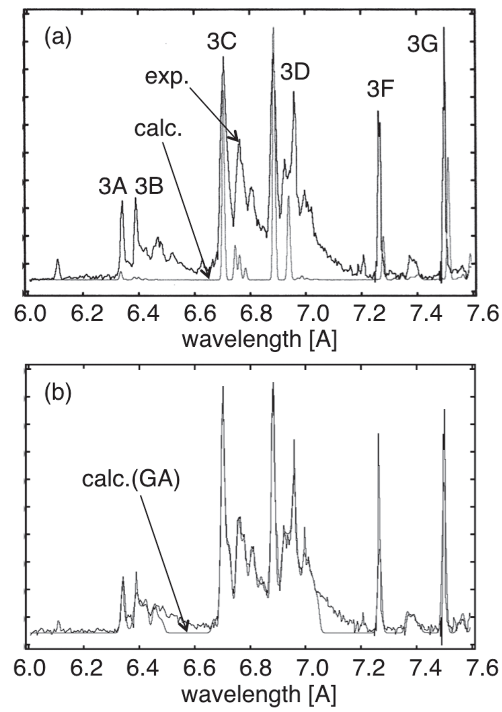

Fig. 5 Emission spectrum of near Ne-like Kr, calculated using (a) only with Ne-like lines without optimization, and (b) including F- and Na-like ions and optimized using GA.

4. Results of Calculation of Kr Spectrum Using Genetic Algorithm (GA)

The study of EUV source has demonstrated that even atomic codes can produce atomic data, the calculated line wavelength contains errors even considering configuration interaction. Furthermore, the line wavelength cannot always be experimentally calibrated [10].

As an another test case in the NLTE7, we analyzed the spectrum from a laser produced Kr plasma [11], using the genetic algorithm (GA) to consider an inverse problem to find level energies and populations that reproduce the spectrum. T_{ion}, T_e, correction of population and energy for each level, Δp_j and ΔE_j, and effective line width and size of the plasma are considered as genes. For instance, we assume that the level population of jth level, N_j is determined as,

$$N_j = \Delta p_j N_g \frac{g_j}{g_g} \exp\left(-\frac{E_j + \Delta E_j}{kT_e}\right), \qquad (1)$$

from the population of the ground state N_g, which is determined from Saha equilibrium at T_{ion}. Then we calculate the intensity of each line and spectrum, taking the effect of opacity into account, and update genes after evaluating fitness with respect to the experimental spectrum. Next we apply selection, crossover and mutation. This procedure is repeated until convergence is obtained.

Figure 5 shows the wavelengths and intensities of resonance lines of Ne-like Kr that agree with the experiment. Over 500 emission lines from F-, Ne-, and Na-like Kr are

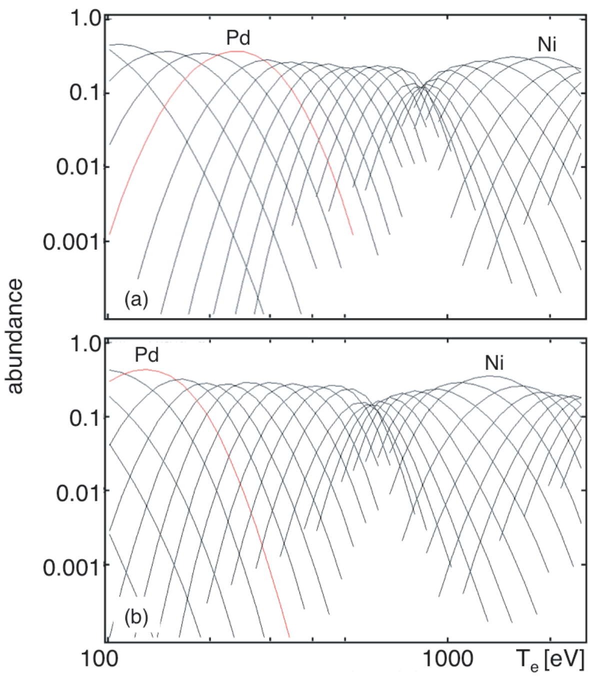

Fig. 6 Abundance curve of (a) Gd and (b) Nd, at an electron density of the plasma of $n_e = 10^{14}/cm^3$.

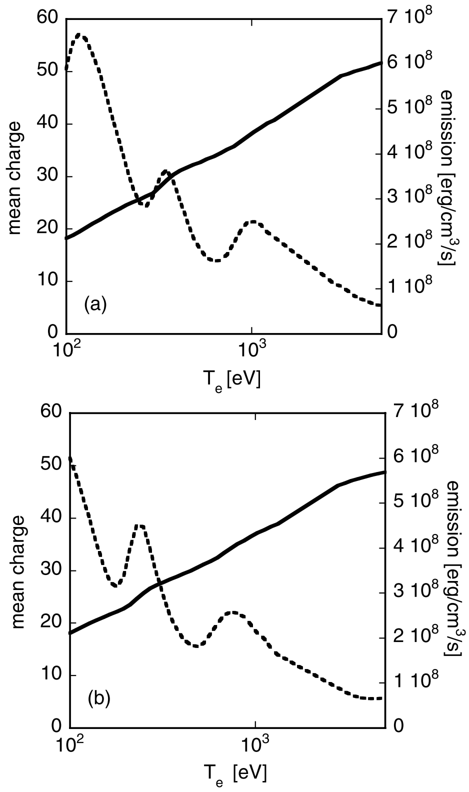

Fig. 7 Mean charge and radiative power loss of (a) Gd and (b) Nd plasmas.

included in the present model, however more satellite lines from Mg- and lower charged Kr ions should be included to improve agreement for the wing of 3A/3B and 3D lines in the longer wavelength region.

5. Application of the JATOM Code to Gd and Nd Plasmas

As an application of JATOM CR code, Fig. 6 shows the ion abundances of Gd and Nd, which is expected to be used for shorter wavelength ($\lambda < 10$ nm) EUV sources [12]. The curves are similar, but are shifted according to the difference of the atomic number. Figure 7 shows the common trend of the radiative power loss, which decreases as temperature increases and number of bound electrons decreases. The dips corresponding to the conditions where the closed shell ion dominates.

6. Summary

The current status of the development and validation of CR model of high-Z ions is described. The modeling method of atomic processes based on computational atomic data and a method based on artificial intelligence will be combined to analyze complex atomic spectra from high-Z plasmas.

[1] see paper presented by Murakami in this proceedings.
[2] *EUV sources for lithography*, edited by V. Bakshi (SPIE press, Bellingham, Washington, U.S.A., 2005).
[3] A. Bar-Shalom, M. Klapisch and J. Oreg, J. Quant. Spectrosc. Radiat. Transf. **71**, 169 (2001).
[4] M.F. Gu, Astrophys. J. **590**, 1131 (2003).
[5] J.G. Rubiano, R. Florido, C. Bowen, R.W. Lee and Yu. Ralchenko, High Energy Density Phys. **3**, 225 (2007).
[6] Yu. Ralchenko *et al.*, AIP Conf. Proc. **1161**, 242 (2009).
[7] http://nlte.nist.gov/NLTE7/
[8] A. Sasaki, accepted for publication in High Energy Density Phys.
[9] T. Pütterich, R. Neu, A.D. Whiteford, M.G. O'Mullane, H.P. Summers and the ASDEX Upgrade Team, Nucl. Fusion **50**, 025012 (2010).
[10] A. Sasaki, A. Sunahara, H. Furukawa, K. Nishihara, S. Fujioka, T. Nishikawa, F. Koike, H. Ohashi and H. Tanuma, J. Appl. Phys. **107**, 113303 (2010).
[11] S. Bastiani-Ceccotti, N. Kontogiannopoulos, J.-R. Marqués, S. Tzortzakis, L. Lecherbourg, F. Thais, I. Matsushima, O. Peyrusse and C. Cenais-Popovics, High Energy Density Phys. **3**, 20 (2007).
[12] B. Li, P. Dunne, T, Higashiguchi, T. Otsuka, N. Yugami, W. Jiang, A. Endo and G. O'Sullivan, Appl. Phys. Lett. **99**, 231502 (2011).